



CHORUS

This is the accepted manuscript made available via CHORUS. The article has been published as:

Hamiltonian theory of fractionally filled Chern bands

Ganpathy Murthy and R. Shankar

Phys. Rev. B **86**, 195146 — Published 30 November 2012

DOI: [10.1103/PhysRevB.86.195146](https://doi.org/10.1103/PhysRevB.86.195146)

Hamiltonian theory of fractionally filled Chern bands

Ganpathy Murthy¹ and R. Shankar²

¹ *Department of Physics and Astronomy, University of Kentucky, Lexington KY 40506-0055*

² *Department of Physics, Yale University, New Haven CT 06520*

There is convincing numerical evidence that fractional quantum Hall-like ground states arise in fractionally filled Chern bands. Here we show that the Hamiltonian theory of Composite Fermions (CF) can be as useful in describing these states as it was in describing the FQHE in the continuum. We are able to introduce CFs into the fractionally filled Chern band problem in two stages. First we construct an algebraically exact mapping which expresses the electron density projected to the Chern band, ρ_{FCB} , as a sum of Girvin-MacDonald-Platzman density operators, ρ_{GMP} , that obey the magnetic translation algebra. Next, following our Hamiltonian treatment of the FQH problem, we rewrite the operators ρ_{GMP} in terms of CF variables which reproduce the same algebra. This naturally produces a unique Hartree-Fock ground state for the CFs, which can be used as a springboard for computing gaps, response functions, temperature-dependent phenomena, and the influence of disorder. We give two concrete examples, one of which has no analog in the continuum FQHE with $\nu = \frac{1}{5}$ and $\sigma_{xy} = \frac{2}{5}$. Our approach can be easily extended to fractionally filled, strongly interacting two-dimensional time-reversal-invariant topological insulators.

PACS numbers:

I. INTRODUCTION

The first examples of bands with a nonzero, and quantized, Hall conductance arose from electrons in a uniform external magnetic field. However, it has since become evident that these are special cases of the more general phenomenon of Chern bands. Lattice¹ and continuum² models with a quantized Hall conductance σ_{xy} and no reference to a uniform external magnetic field were identified in the late 80's. In a Chern band, the breaking of time-reversal symmetry, necessary for $\sigma_{xy} \neq 0$, manifests itself as a nontrivial Berry flux for the band, whose non-zero integral over the Brillouin zone (BZ) gives the Chern number \mathcal{C} . The work of Thouless *et al.*³, relates \mathcal{C} to the dimensionless Hall conductance of the filled band. We use a convention in which $\sigma_{xy} = -\mathcal{C}$.

While we focus on single Chern bands, the approach to be described here readily applies to strongly interacting two dimensional time-reversal invariant topological insulators^{4,5} which can be thought of as pairs of time reversed Chern bands.

A question that has recently attracted much attention is whether these Chern bands could also exhibit the FQHE at fractional filling in the presence of suitable interactions. In such cases they are called Fractional Chern Insulators. Optimal (but not perhaps strictly necessary) conditions call for a hierarchy of scales, where the band gap Δ , the interaction strength V_{ee} , and the bandwidth W obey $\Delta \gg V_{ee} \gg W$.

There have been three fronts of attack. Numerical efforts have concentrated on “flattening” the Chern band⁶⁻⁸, and realized Laughlin-like states⁹ by exact diagonalization^{8,10-13}. Most recently, other principal FQH fractions such as $2/5$ and $3/7$ have been seen as well¹⁴. On the analytical front, Qi¹⁵ has constructed a basis in which known FQHE wavefunctions can be transcribed into the Chern band. Subsequently Wu, Regnault and Bernevig¹⁶ have pointed out ways to improve Qi's results by exploiting the residual gauge freedom in

the choice of basis. Considerable effort has also been devoted to the parton construction for fractional Chern insulators¹⁷⁻¹⁹ in which the electron is fractionalized into quarks, each of which is in an integer quantum Hall state.

Our work was stimulated by the third approach due to Parameswaran *et al.*²⁰, who examined the algebra of $\rho_{\text{FCB}}(\mathbf{q})$, the density operators projected into the fractionally filled Chern band (FCB). Recall that in the Lowest Landau Level (LLL) problem the projected density is essentially $\rho_{\text{GMP}}(\mathbf{q})$, the Girvin-MacDonald-Platzman²¹ (GMP) operator, which obeys the algebra of magnetic translations:

$$[\rho_{\text{GMP}}(\mathbf{q}), \rho_{\text{GMP}}(\mathbf{q}')] = 2i \sin \left[\frac{l^2}{2} \mathbf{q} \times \mathbf{q}' \right] \rho_{\text{GMP}}(\mathbf{q} + \mathbf{q}'). \quad (1)$$

where

$$l = \frac{1}{\sqrt{eB_0}} \quad (2)$$

is the magnetic length associated with the perpendicular external field B_0 . This algebra was exploited to great effect by GMP in their study of collective modes. By contrast, the algebra of $\rho_{\text{FCB}}(\mathbf{q})$ does not even close²⁰, though in the small \mathbf{q}, \mathbf{q}' limit the commutator is proportional to $\mathbf{q} \times \mathbf{q}'$. The fundamental reason for the non-closure of the density algebra is the varying Chern density $\mathcal{B}(\mathbf{p})$ in the Brillouin Zone (BZ). Parameswaran *et al.* offer interesting ways to combat the varying \mathcal{B} , such as smoothing it out or replacing it by its average²⁰.

Our main contribution here is to show that in our Hamiltonian approach²², given any Chern band- whether it originates from a Landau level problem or a lattice model²³, and no matter how $\mathcal{B}(\mathbf{p})$ varies- we may introduce CFs²⁴ and that they will once again single out gapped states at special fillings and permit the computation of various correlation functions at non zero \mathbf{q}, ω and T . This is possible because of the way we introduce

CFs in the FQHE. It differs from the wavefunction approach of singular gauge transformations²⁵ as adapted by Jain²⁴, and the Chern-Simons theory along the lines of Zhang, Hansson and Kivelson²⁶ (who expressed the theory in terms of composite bosons) or Lopez and Fradkin²⁷ who rewrote the theory in terms of composite fermions. In the Hamiltonian approach²², we focus on $\rho_{\text{GMP}}(\mathbf{q})$, the Girvin-MacDonald-Platzman²¹ density operator in terms of which the hamiltonian in the LLL problem may be written (on dropping the constant kinetic energy of the LLL) as

$$H_{\text{LLL}} = \frac{1}{2} \sum_{\mathbf{q}} \rho_{\text{GMP}}(\mathbf{q}) \rho_{\text{GMP}}(-\mathbf{q}) v(q) e^{-q^2 l^2 / 2}. \quad (3)$$

Instead of writing $\rho_{\text{GMP}}(\mathbf{q})$ in terms of the electron guiding center coordinate \mathbf{R}_e , we express it in terms of the guiding center and cyclotron coordinates of a CF which experience a weaker field than the electron, exactly as in the usual wavefunction-based CF treatments. While the algebra of $\rho_{\text{GMP}}(\mathbf{q})$ is replicated in the enlarged Hilbert space, the macroscopic ground state degeneracy at fractional filling is removed since the CFs have a natural gapped ground state in which they fill an integer number of Composite Fermion Landau Levels, or CF-LLs.

Having a theory expressed in terms of CFs is very useful in the FQH regime for many reasons: Even though the electrons are strongly correlated, the CFs are in states that are weakly correlated, in the sense that they are treatable by standard many-body approximations such as Hartree-Fock. Let us also recall that the utility of CFs goes beyond gapped states, and applies to the Fermi-liquid-like state at $\nu = \frac{1}{2}$ ²⁸⁻³⁰.

Our approach²², which has the virtue of allowing the computation of not only gaps but also non-trivial response functions, is applicable to the current problem of fractionally filled Chern bands. Two results we establish are key to applying the Hamiltonian approach in this problem:

- Given canonical creation and destruction operators $d^\dagger(\mathbf{p})$ and $d(\mathbf{p})$ from any band with any lattice symmetry, we can form objects that obey the same algebra as $\rho_{\text{GMP}}(\mathbf{q})$, where \mathbf{q} is not restricted to the BZ.
- The electron density operator projected to the fractionally filled Chern band (abbreviated FCB), $\rho_{\text{FCB}}(\mathbf{Q})$, where $\mathbf{Q} \in \text{BZ}$, and the kinetic energy may be expressed as linear combinations of the above mentioned GMP densities at $\mathbf{Q} + \mathbf{G}$, where \mathbf{G} is any reciprocal lattice vector, with coefficients $c(\mathbf{G}, \mathbf{Q})$ that are easily computed as Fourier coefficients.

It is then a simple matter to rewrite every $\rho_{\text{GMP}}(\mathbf{Q} + \mathbf{G})$ in the sum in terms of CF variables and proceed with standard many-body approximations. The rest of this paper will flesh out the key results above and give examples of their application.

Our paper is organized as follows. In Section II, we recall the notion of a Chern band and state the problem of the fractionally filled Chern band for the benefit of the non-experts who we hope to draw into this problem. In Section III we study the oldest Chern band, the LLL, and explain how the Hamiltonian theory is applied to the familiar FQHE in the continuum. Section IV states and proves our central claim, that given any band in a two-dimensional crystal, one can construct operators that obey the magnetic translation algebra, and that these operators form a complete set. Thus, the electron density projected to the Chern band can be expressed as a sum over GMP operators. Section V describes in some detail how we implement this technology in the fractionally filled Chern band problem. We show the results from Hartree-Fock calculations for a $\nu = \frac{1}{3}$ -filled Chern band arising from a problem involving two Landau levels in a periodic potential. We also show how one should proceed given a lattice model, using the lattice Dirac model as an example. Section VI discusses the possibility of observing the FQHE in band with zero Chern number. In Section VIII we present results on a state that is possible only on a lattice. These are states where the filling fraction is not equal to the dimensionless Hall conductance: $\nu = \frac{1}{5}$ and $\sigma_{xy} = \frac{2}{5}$, and arise from the explicit breaking of Galilean invariance. They are concrete realizations of Chern-Simons theories in the presence of a periodic potential³¹⁻³³, but can also be thought of as Hall Crystals³⁴ stabilized by the lattice. Conclusions and discussion follow in Section VIII.

II. THE FRACTIONALLY FILLED CHERN BAND PROBLEM

A Chern band is a concept applicable to non-interacting systems, an example of which is the lattice Dirac model:

$$\begin{aligned} H(\mathbf{p}) &= \sigma_1 \sin p_x + \sigma_2 \sin p_y + \sigma_3 (M - \cos p_x - \cos p_y) \\ &\equiv \boldsymbol{\sigma} \cdot \mathbf{h}(\mathbf{p}) \end{aligned} \quad (4)$$

where \mathbf{p} is a momentum in the BZ and $\boldsymbol{\sigma}$ are the Pauli matrices and M is a free parameter. At each \mathbf{p} the eigenvalue equation for the Bloch spinor

$$H(\mathbf{p})u(\mathbf{p}) = \varepsilon(\mathbf{p})u(\mathbf{p}) \quad (5)$$

has two solutions

$$\varepsilon(\mathbf{p}) = \pm |\mathbf{h}|. \quad (6)$$

Focus on the lower band and follow the down spinor $u(\mathbf{p})$ as \mathbf{p} varies over the BZ. The expectation value

$$\mathbf{n}(\mathbf{p}) = u^\dagger \boldsymbol{\sigma} u \quad (7)$$

lies on the unit sphere and the number of times the BZ wraps around this target sphere is the winding number \mathcal{W} and it equals \mathcal{C} the Chern number. If M is very large

the spinor will get stuck at one of the poles for all \mathbf{p} and \mathcal{C} will vanish. It turns out that M has to lie in a limited range for non-trivial topology. We will work with $M = 1$, for which $\mathcal{C} = -1$.

While the above approach is adequate for a two-band model, the more general way to define the Chern density is as follows: Given the Bloch functions $|u(\mathbf{p})\rangle$ of the band of interest, first define the Berry connection

$$\mathcal{A}(\mathbf{p}) = i\langle u(\mathbf{p})|\nabla_p|u(\mathbf{p})\rangle \quad (8)$$

Then the Berry curvature or Chern flux density is

$$\mathcal{B}(\mathbf{p}) = \nabla_p \times \mathcal{A} \quad \text{in terms of which} \quad (9)$$

$$\mathcal{C} = \frac{1}{2\pi} \int_{BZ} \mathcal{B}. \quad (10)$$

A Chern band has non-zero \mathcal{C} .

Without interactions two things are certain: if the band is filled it will have a dimensionless Hall conductance $\sigma_{xy} = -\mathcal{C}$ and if it is partially filled, it will be a Fermi liquid.

At partial filling we need interactions if we want a different answer. Abbreviating fractionally filled Chern band as FCB, the Hamiltonian to solve is

$$H_{FCB} = \sum_{\mathbf{p} \in BZ} d^\dagger(\mathbf{p})d(\mathbf{p})(-\varepsilon(\mathbf{p})) \quad (11)$$

$$+ \frac{1}{2} \sum_{\mathbf{q}} \rho_{FCB}(\mathbf{q})\rho_{FCB}(-\mathbf{q})v(q) \quad (12)$$

where $\rho_{FCB}(\mathbf{q})$ is the density projected to the Chern band and $v(q)$ the electron-electron interaction. We cannot do weak coupling perturbation theory around the Fermi liquid if we want to see the FQHE and we cannot resort to the Hartree-Fock approximation because no unique gapped state emerges in the electron variables at fractional filling. We do not have analyticity as we did in the LLL, which together with antisymmetry pointed to the Laughlin fractions for $\nu = \frac{1}{2s+1}$.

Clearly, to pick out the FQH-like states we need to express the Hamiltonian in CF variables. To this end we recall how they were introduced by us in the usual continuum FQHE.

III. THE OLDEST CHERN BAND: THE LLL

Working back from the result $\sigma_{xy} = 1$ in the LLL we may conclude it has $\mathcal{C} = -1$. (The minus sign simply reflects our convention.) Let us ask how we can show that. (We recommend the review by Xiao, Chang and Niu for some basic ideas of magnetic Bloch bands³⁵.)

First we mentally superpose on the continuum two-dimensional electron gas immersed in a perpendicular field B_0 , a square lattice of side a (the square lattice is the simplest case; as will be evident in the following, we can start with any lattice whatsoever). No real periodic

potential is applied yet. Working in the Landau gauge where the vector potential has components

$$A_y(x, y) = xB_0 \quad A_x(x, y) = 0 \quad (13)$$

we seek energy eigenfunctions which are also simultaneous eigenfunctions of T_x and T_y , the magnetic translation operators in the x and y directions:

$$T_x = e^{-iaye\ell^{-2}} e^{a\partial_x} \quad T_y = e^{a\partial_y}. \quad (14)$$

These commute with H , but not with each other unless each unit cell has an integer number of flux quanta. We choose the simplest case of one flux quantum penetrating each unit cell, i.e.,

$$a^2 = 2\pi\ell^2. \quad (15)$$

The simultaneous eigenfunctions we seek are³:

$$\langle x_e, y_e | \mathbf{p}, n \rangle = \Psi_{\mathbf{p}, n}(x_e, y_e) \quad (16)$$

$$= \frac{1}{\sqrt{a}} \sum_{j=-\infty}^{\infty} e^{iy_e(p_y + aj\ell^{-2})} e^{iap_x j} \phi_n(x_e - aj - p_y\ell^2) \quad (17)$$

where $\phi_n(x_e - aj - p_y\ell^2)$ is the wavefunction for an oscillator in level n centered at $x_e = aj + \ell^2 p_y$.

Hereafter we will set $a = 1$ which means

$$\ell^2 = \frac{1}{2\pi}. \quad (18)$$

The states are normalized to unity, and \mathbf{r}_e integrals go over the spatial unit cell. The Bloch functions are

$$|u(\mathbf{p}, n)\rangle = e^{-i\mathbf{p}\cdot\mathbf{r}_e} |\mathbf{p}, n\rangle \quad (19)$$

and the Berry connection

$$\mathcal{A}(\mathbf{p}, n) = i\langle u(\mathbf{p}, n)|\nabla_p|u(\mathbf{p}, n)\rangle \quad (20)$$

can be computed to have components

$$\mathcal{A}_y = 0 \quad \mathcal{A}_x = p_y\ell^2 = \frac{1}{2\pi}p_y \quad \text{so that} \quad (21)$$

$$\mathcal{B}(\mathbf{p}) = \nabla_p \times \mathcal{A} = -\frac{1}{2\pi} \quad \text{which means} \quad (22)$$

$$\mathcal{C} = \frac{1}{2\pi} \int_{BZ} \mathcal{B} = -1. \quad (23)$$

The Hamiltonian in the LLL was referred to earlier:

$$H_{LLL} = \frac{1}{2} \sum_{\mathbf{q}} \rho_{GMP}(\mathbf{q})\rho_{GMP}(-\mathbf{q})v(q)e^{-q^2\ell^2/2}. \quad (24)$$

Let us now obtain this projected Hamiltonian and $\rho_{GMP}(\mathbf{q})$ form the original electronic problem. Start with

the standard expression for the electron density operator in the full Hilbert space (including all Landau levels) in first quantization:

$$\rho(\mathbf{q}) = \sum_j e^{i\mathbf{q}\cdot\mathbf{r}_e}. \quad (25)$$

The electron's position \mathbf{r}_e may be decomposed as

$$\mathbf{r}_e = \mathbf{R}_e + \boldsymbol{\eta}_e \quad (26)$$

where the electronic guiding center coordinate $\mathbf{R}_e = \mathbf{r}_e - \boldsymbol{\eta}_e$, and where the cyclotron coordinate $\boldsymbol{\eta}_e$ is in turn defined as

$$\boldsymbol{\eta}_e = l^2 \mathbf{z} \times \boldsymbol{\Pi}_e = l^2 \mathbf{z} \times (\mathbf{p}_e - \mathbf{A}(\mathbf{r}_e)). \quad (27)$$

Here $\mathbf{A}(\mathbf{r}_e)$ is the vector potential of the external magnetic field, not to be confused with the Berry connection \mathcal{A} . The coordinates $\boldsymbol{\eta}_e$, \mathbf{R}_e satisfy the commutation relations

$$[R_{ex}, R_{ey}] = -il^2 \quad (28)$$

$$[\eta_{ex}, \eta_{ey}] = il^2 \quad (29)$$

$$[\boldsymbol{\eta}_e, \mathbf{R}_e] = 0. \quad (30)$$

Upon projecting the electron density operator to the LLL we obtain

$$\rho_{\text{LLL}}(\mathbf{q}) = \sum_j \langle e^{i\mathbf{q}\cdot\boldsymbol{\eta}_{ej}} \rangle_{\text{LLL}} e^{i\mathbf{q}\cdot\mathbf{R}_{ej}} = e^{-q^2 l^2 / 4} \rho_{\text{GMP}}(\mathbf{q}) \quad (31)$$

where each term $e^{i\mathbf{q}\cdot\mathbf{R}_{ej}}$ in the sum obeys the GMP algebra by itself thanks to Eq. 28. We shall use the same symbol for the densities when we switch to second quantization.

The cyclotron coordinate enters the non-interacting Hamiltonian:

$$H_0 = \frac{(\mathbf{p}_e - e\mathbf{A}(\mathbf{r}_e))^2}{2m} = \frac{\boldsymbol{\eta}_e^2}{2ml^4} \quad (32)$$

while the guiding center coordinate \mathbf{R}_e , which is a cyclic coordinate, explains the degeneracy of the LLL. Since \mathbf{r}_e can roam over the sample of area A and $|\boldsymbol{\eta}_e| \simeq l$, \mathbf{R}_e can roam over the sample area. Since R_{ex} and R_{ey} are conjugate variables, and l^2 plays the role of \hbar , the sample is the phase space for \mathbf{R}_e and the number of states in a LL is

$$\frac{A}{\hbar} = \frac{A}{2\pi l^2} = \frac{eAB_0}{2\pi} = \frac{\Phi}{\Phi_0} = N_\Phi \quad (33)$$

which is the total flux in units of flux quantum $\Phi_0 = 2\pi/e$ (with the real $\hbar = 1$). If N_e is the number of electrons, the filling fraction is $\nu = N_e/N_\Phi$ and its inverse is the number of single particle states or flux quanta per electron. For $\nu < 1$, we face a macroscopic degeneracy trying to fill N_Φ states with $N_e < N_\Phi$ electrons.

The CF idea of Jain²⁴ for $\nu = p/(2p+1)$ is to attach two flux quanta per electron to form the CFs. The number of electrons is the same as the number of CFs, but

the number of effective flux quanta seen by the CFs is $N_\Phi^* = N_\Phi - 2N_e$ which leads to the CF filling factor

$$(\nu^*)^{-1} = \frac{N_\Phi^*}{N_e} = \nu^{-1} - 2 = \frac{1}{p} \quad (34)$$

Thus, the CFs fill p CF-LLs. (Jain's approach applies²⁴ in general to $\nu = p/(2ps+1)$, where $2s$ flux quanta are attached, but we focus on $s = 1$ to illustrate our ideas.)

We, too, embrace the idea of the CF that sees just the right field to fill p CF-LLs, but implement it in an operator-based approach as follows. We introduce a Hilbert space for a CF which sees the field $B^* = \frac{B_0}{2p+1}$ that the CF of reduced charge $e^* = \frac{e}{2p+1}$ is supposed to see in Jain's picture. This information is encoded in the algebra of its cyclotron $\boldsymbol{\eta}$ and guiding center \mathbf{R} coordinates (which do not carry the subscript e) and obey

$$[\eta_x, \eta_y] = il^{*2} = i \frac{l^2}{1-c^2} \quad (35)$$

$$[R_x, R_y] = -il^{*2} \quad (36)$$

$$[\boldsymbol{\eta}, \mathbf{R}] = 0 \quad (37)$$

$$c^2 = 2\nu = \frac{2p}{2p+1} \quad (38)$$

It is readily verified that the combination

$$\mathbf{R}_e = \mathbf{R} + \boldsymbol{\eta} c \quad (39)$$

$$(40)$$

obeys

$$[R_{ex}, R_{ey}] = -il^2. \quad (41)$$

This in turn permits the crucial *CF substitution*

$$\rho_{\text{GMP}}(\mathbf{q}) = \sum_j \exp[i\mathbf{q} \cdot (\mathbf{R}_j + c\boldsymbol{\eta}_j)] \quad (42)$$

in Eqn. 24 for the projected Hamiltonian H_{LLL} , which now acts on a regular fermionic Hilbert space with two conjugate pairs per particle. Since the CFs see exactly the right field to fill p CF-LLs, a natural, gapped Hartree-Fock state emerges.

There is a catch. Using \mathbf{R} and $\boldsymbol{\eta}$ we can form a second conjugate pair

$$\mathbf{R}_v = \mathbf{R} + \boldsymbol{\eta}/c \quad (43)$$

called the pseudovortex coordinate, obeying

$$[R_{vx}, R_{vy}] = i \frac{l^2}{c^2} \quad (44)$$

$$[\mathbf{R}_e, \mathbf{R}_v] = 0. \quad (45)$$

It has no dynamics and commutes with $H_{\text{LLL}}(\mathbf{R}_e)$.

We call it the pseudovortex coordinate because it has the same charge as the double vortex that is supposed to bind with the electron to form the CF in the wavefunction approach. The price we pay for obtaining a

good mean-field starting point is that our Hilbert space has these unphysical degrees of freedom \mathbf{R}_v . In order to work in the physical sector the vortex coordinates need to be constrained. Specifically, the vortex densities, $\rho_v(\mathbf{q}) = e^{i\mathbf{q}\cdot\mathbf{R}_v}$, emerge as a gauge algebra. The way to handle this gauge degree of freedom is described in our review²².

The Hamiltonian is a function of \mathbf{R}_e alone, and thus any function of the \mathbf{R}_v commutes with the Hamiltonian. This has the following important consequence:

The energy of any trial state in the enlarged Hilbert space provides a variational upper bound on the true ground state energy.

To see this note that the exact ground state in the enlarged space is a tensor product of the exact ground state in the physical space (of \mathbf{R}_e) and an arbitrary state in the \mathbf{R}_v sector. Since H is independent of \mathbf{R}_v , the ground state energy in the enlarged Hilbert space is identical to the exact ground state energy. The variationality of ground state energy in the enlarged space follows. We will use this fact to investigate the relative stability of electronic versus CF ground states in what follows.

We have computed many physical quantities in this Hamiltonian approach in the continuum FQH regime²². We find semiquantitative agreement with numerical results for gaps³⁶. Response functions can be computed in a conserving approximation (which approximately projects to the physical space) and qualitatively correct results for the static structure factor of incompressible states are obtained³⁷. With the introduction of the layer thickness as a single fitting parameter, experimental spin polarizations for 1/3 and 1/2 can be reproduced over the entire temperature range to within a few percent³⁸. Furthermore, disorder can also be handled in this formalism, leading to good agreement with data on NMR relaxation time³⁹ as a function of total field at $\nu = 1/2$, and gaps as a function of total field⁴⁰ at $\nu = 1/3$.

The key point, going forward, is this: once the problem is written in terms of $\rho_{\text{GMP}}(\mathbf{q})$ we can make the CF substitution and go on to standard many-body approximations for single-particle as well as collective properties.

IV. THE CHERN BAND IN TERMS OF $\rho_{\text{GMP}}(\mathbf{q})$

We will now show how the entire Chern band Hamiltonian can be expressed in terms of GMP densities. First let us go back to the electrons in the continuum, on which a periodic ‘‘empty’’ lattice was mentally imposed, leading to the symmetry-adapted wavefunctions of Eq. (17). Denoting the electron creation and destruction operators in the BZ as $c_n^\dagger(\mathbf{p})$, $c_n(\mathbf{p})$, we can express $\rho_{\text{GMP}}(\mathbf{q})$ in the LLL in second quantization as

$$\rho_{\text{GMP}}(\mathbf{q}) = \sum_{\mathbf{p}} c_0^\dagger(\mathbf{p}') c_0(\mathbf{p}) e^{i\Phi(\mathbf{q}, \mathbf{p})} \quad \text{where} \quad (46)$$

$$e^{i\Phi(\mathbf{q}, \mathbf{p})} = \langle \mathbf{p}' | e^{i\mathbf{q}\cdot\mathbf{R}_e} | \mathbf{p} \rangle \quad (47)$$

where the subscript 0 denotes the $n = 0$ Landau level, and where the final state momentum \mathbf{p}' is $\mathbf{p} + \mathbf{q}$ brought

back to the BZ (we have introduced the notation $[\mathbf{p} + \mathbf{q}]$ for this)

$$\mathbf{p}' \equiv [\mathbf{p} + \mathbf{q}] = \mathbf{p} + \mathbf{q} - \mathbf{e}_x 2\pi N_x - \mathbf{e}_y 2\pi N_y. \quad (48)$$

The matrix element of Eq. 47 is

$$e^{i\Phi(\mathbf{q}, \mathbf{p})} = \exp \left[\frac{i}{2\pi} \left(\frac{1}{2} q_x q_y + q_x p_y - (p_x + q_x) 2\pi N_y \right) \right] \quad (49)$$

It is important to note that \mathbf{q} is not restricted to the BZ. While the above is special to the square lattice, it is evident that a similar construction can be performed for any lattice.

Now, let us consider any given band on a square lattice with canonical destruction and creation operators $d(\mathbf{p})$, $d^\dagger(\mathbf{p})$. Let us construct the following operator with momentum \mathbf{q} *not necessarily in the BZ*

$$\begin{aligned} \rho_{\text{GMP}}(\mathbf{q}) &= \sum_{\mathbf{p} \in \text{BZ}_e} d^\dagger(\mathbf{p}') d(\mathbf{p}) e^{i\Phi(\mathbf{q}, \mathbf{p})} \quad (50) \\ &= \sum_{\mathbf{p} \in \text{BZ}_e} d^\dagger(\mathbf{p}') d(\mathbf{p}) \\ &\times \exp \left[\frac{i}{2\pi} \left(\frac{1}{2} q_x q_y + q_x p_y - (p_x + q_x) 2\pi N_y \right) \right] \quad (51) \end{aligned}$$

We call this operator $\rho_{\text{GMP}}(\mathbf{q})$ because it obeys the algebra of the GMP densities since all it takes is the right coefficient $e^{i\Phi}$ and canonical commutation rules of d and d^\dagger . It does not matter that they do not come from a Landau Level. Once again, \mathbf{q} is not restricted to the BZ. In a purely lattice problem the momentum transfer \mathbf{Q} will also be restricted to the BZ, so let us decompose

$$\mathbf{q} = \mathbf{Q} + \mathbf{G} = \mathbf{Q} + 2\pi n_x \mathbf{e}_x + 2\pi n_y \mathbf{e}_y : \quad (52)$$

leading to

$$\begin{aligned} \rho_{\text{GMP}}(\mathbf{Q} + \mathbf{G}) &= \sum_{\mathbf{p}} d^\dagger(\mathbf{p}') d(\mathbf{p}) e^{i\Phi(\mathbf{Q} + \mathbf{G}, \mathbf{p})} \\ &= \sum_{\mathbf{p}} d^\dagger(\mathbf{p}') d(\mathbf{p}) e^{i\Phi(\mathbf{Q}, \mathbf{p})} e^{\frac{i}{2}(Q_y n_x - Q_x n_y + 2\pi n_x n_y)} e^{-ip_x n_y + ip_y n_x} \quad (53) \end{aligned}$$

Clearly, adding \mathbf{G} to \mathbf{Q} does not affect the values of \mathbf{p} , \mathbf{p}' , but does affect the phase factor in the sum.

Now we are ready to state our central claim. The electron density operator projected to the fractionally filled Chern band (FCB) can be expressed as

$$\rho_{\text{FCB}}(\mathbf{Q}) = \sum_{\mathbf{G}} c(\mathbf{G}, \mathbf{Q}) \rho_{\text{GMP}}(\mathbf{Q} + \mathbf{G}) \quad (54)$$

where the coefficients $c(\mathbf{G}, \mathbf{Q})$ can be computed from the data on the original Chern band, essentially by Fourier transformation. The CF-substitution can be then made in each $\rho_{\text{GMP}}(\mathbf{Q} + \mathbf{G})$.

Indeed we will show that we can expand *any* bilinear of the form $d^\dagger d$ in terms of $\rho_{\text{GMP}}(\mathbf{Q} + \mathbf{G})$. The reason is that there are as many independent operators $\rho_{\text{GMP}}(\mathbf{Q} + \mathbf{G})$ as there are bilinears $d^\dagger(\mathbf{p}_2)d(\mathbf{p}_1)$ in the canonical basis.

To count the number of linearly independent operators we need to consider a finite system, which we choose to be a torus of size $L \times L$. Firstly, it is clear that ρ_{GMP} for *different* values of $\mathbf{Q} \in BZ$ are linearly independent. So the question becomes, for a given $\mathbf{Q} \in BZ$, for how many different values of \mathbf{G} are the $\rho_{\text{GMP}}(\mathbf{Q} + \mathbf{G})$ linearly independent? Since $a = 1$, the number of sites is $N^2 = \frac{L^2}{a^2} = L^2$, which also equals the number of points in the BZ. Clearly, N^2 is the number of distinct values for the single-particle momentum $\mathbf{p} \in BZ$, and the number of distinct values of $\mathbf{Q} \in BZ$ in the lattice model. The smallest value for any component of \mathbf{Q} or \mathbf{p} is $Q_{\min} = p_{\min} = \frac{2\pi}{L}$.

Now we demonstrate that adding $2\pi N\hat{e}_x$ or $2\pi N\hat{e}_y$ to \mathbf{Q} in ρ_{GMP} does not lead to a linearly independent expression.

To verify this consider the second and third exponentials in Eq. 53 which alone depend on \mathbf{G} . Focus on a factor like $e^{-\frac{i}{2}Q_x n_y}$ when $Q_x = Q_{\min}$ and $n_y = N$

$$e^{-\frac{i}{2}q_x n_y} \Big|_{q_x = \frac{2\pi}{L}, n_y = N} = e^{-i\pi \frac{N}{L}} = -1. \quad (55)$$

The same goes for all the terms in the second exponential, while the third exponential always equals unity, which means

$$\rho_{\text{GMP}}(\mathbf{q} + \mathbf{G}_{\max}) \propto \rho_{\text{GMP}}(\mathbf{q}) \quad (56)$$

It is easy to see that this linear dependence holds for any value of \mathbf{Q} .

Thus we get linearly independent densities only for components up to $G_{\max} = 2\pi N$. There are only N^2 independent values of \mathbf{G} , just as for \mathbf{p} or \mathbf{Q} . But this means there are N^4 linearly independent operators of the form $\rho_{\text{GMP}}(\mathbf{Q} + \mathbf{G})$, exactly the right number to form a basis, like the canonical basis $d_{\mathbf{p}_2}^\dagger d_{\mathbf{p}_1}$. So what we find is that not only ρ_{FCB} , but any bilinear operator O (such as the lattice current operator) of the form $\sum_{\mathbf{p}} d^\dagger(\mathbf{p}')d(\mathbf{p})O(\mathbf{Q}, \mathbf{p})$ can be expanded in terms of $\rho_{\text{GMP}}(\mathbf{Q} + \mathbf{G})$.

Now consider the proposed expansion $\rho_{\text{FCB}}(\mathbf{Q})$ in terms of $\rho_{\text{GMP}}(\mathbf{Q} + \mathbf{G})$:

$$\begin{aligned} & \sum_{\mathbf{p}} d^\dagger(\mathbf{p}')d(\mathbf{p})e^{i\Phi(\mathbf{Q} + \mathbf{G}, \mathbf{p})} \\ &= \sum_{\mathbf{p}} d^\dagger(\mathbf{p}')d(\mathbf{p})e^{i\Phi(\mathbf{Q}, \mathbf{p})} e^{\frac{i}{2}(Q_y n_x - Q_x n_y + 2\pi n_x n_y)} e^{ip_y n_x - ip_x n_y} \end{aligned}$$

This amounts to a Fourier expansion of $f(\mathbf{Q}, \mathbf{p})$:

$$\begin{aligned} f(\mathbf{Q}, \mathbf{p}) &= \sum_{n_x, n_y} c(n_x, n_y, \mathbf{Q}) \\ &\times e^{\frac{i}{2}(-Q_x n_y + Q_y n_x + 2\pi n_x n_y)} e^{-ip_x n_y + ip_y n_x} \end{aligned} \quad (58)$$

is, at each \mathbf{Q} , just the Fourier expansion of the function f periodic in \mathbf{p} in terms of oscillating exponentials of the right period.

Since $f(\mathbf{Q}, \mathbf{p})$ was not anything special above, the result holds for any bilinear. The expansion of the kinetic term is a special case of $\mathbf{Q} = 0$:

$$\begin{aligned} & \sum_{\mathbf{p}} d^\dagger(\mathbf{p})d(\mathbf{p})(-\varepsilon(\mathbf{p})) \\ &= \sum_{\mathbf{G}} h(\mathbf{G})\rho_{\text{GMP}}(\mathbf{G}) \\ &= \sum_{n_x n_y \mathbf{p}} d^\dagger(\mathbf{p})d(\mathbf{p})h(n_x, n_y)e^{-ip_x n_y + ip_y n_x + i\pi n_x n_y} \end{aligned} \quad (59)$$

which amounts to Fourier expanding the energy dispersion $-\varepsilon(\mathbf{p})$. We now have the full electronic Hamiltonian for the FCB in terms of ρ_{GMP} . We are now ready to perform the CF substitution and the Hartree-Fock approximation.

V. COMPOSITE FERMION SUBSTITUTION AND THE HARTREE-FOCK APPROXIMATION

We have found two ways to demonstrate our method which differ only in the way the Chern band is introduced.

In the first subsection we couple two LL's with a periodic potential and use the lower band as the Chern band. It should be clear by now that once you have a Chern band it does not matter where it came from. Our reason for using this version is that the expansion of ρ_{FCB} in terms of ρ_{GMP} converges very rapidly. This is the case for which we display the results of the Hartree Fock calculation for $\nu = \frac{1}{3}$ and $\nu = \frac{1}{5}$, (with $\sigma_{xy} = \frac{2}{5}$.)

In the final subsection we consider the lower band of the lattice Dirac model at $M = 1$ when $\mathcal{C} = -1$. Here we show how a satisfactory expansion of ρ_{FCB} in terms of ρ_{GMP} obtains. No Hartree Fock results are presented for this model, since these have not yet been carried out.

A. Landau Level based models

The goal of this section is to convince the reader that a nonconstant $\mathcal{B}(\mathbf{p})$ is no impediment to the CF substitution, and to flesh out the key expansion Eq. 54. We begin with the construction of a nontrivial Chern band with a non-constant $\mathcal{B}(\mathbf{p})$.

Consider a problem with two LLs labeled 0 and 1 separated by a gap ω that is at our disposal, as shown in Fig.1. By choosing the Hamiltonian to be a suitable function of $\boldsymbol{\eta}_e^\dagger \boldsymbol{\eta}_e$, not simply linear, we can arrange for the

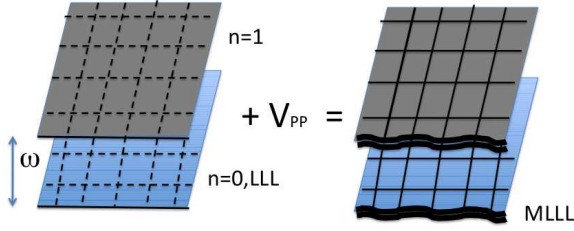


FIG. 1: Left: Two unperturbed Landau Levels with $\mathcal{C} = -1$ and zero width separated by energy ω . The dotted grid represents a fictitious square lattice with one flux quantum per unit cell. Right: The two bands with finite width after a periodic potential V_{PP} (solid grid) is imposed. The lower of the two bands is our Chern band with $\mathcal{C} = -1$.

other LLs to be separated by a parametrically larger gap than ω and hence ignorable in what follows.

Each level has $\mathcal{C} = -1$. However the Chern density \mathcal{B} is constant in \mathbf{p} in both LLs. To make it vary, we add a periodic potential

$$V(\mathbf{r}_e) = \sum_{\mathbf{G}} V(\mathbf{G}) e^{i\mathbf{G} \cdot \mathbf{r}_e} \quad (61)$$

which mixes the LLs, bequeaths a bandwidth and induces structure in $\mathcal{B}(\mathbf{p})$. In our illustrative example we keep only the harmonics $\pm 2\pi$ in the two directions with coefficient V_{10} , though the following analysis applies to the general case. Using

$$\langle \mathbf{p}n_2 | e^{i\mathbf{G} \cdot \mathbf{r}} | \mathbf{p}n_1 \rangle = \rho_{n_2 n_1} e^{iG_x G_y / 4\pi} e^{i\mathbf{G} \times \mathbf{p} / 2\pi} \quad (62)$$

where (for the general value of l),

$$\begin{aligned} \rho_{n_2 n_1}(\mathbf{q}) &= e^{-q^2 l^2 / 4} \sqrt{\frac{n_{<}!}{n_{>}!}} L_{n_{<}}^{|n_1 - n_2|} \left[\frac{q^2 l^2}{2} \right] \\ &\times \begin{cases} \left(\frac{i l z}{\sqrt{2}} \right)^{|n_1 - n_2|} & \text{when } n_1 > n_2 \\ \left(\frac{i l z}{\sqrt{2}} \right)^{|n_1 - n_2|} & \text{when } n_2 \geq n_1 \end{cases} \\ z &= q_x + i q_y \end{aligned} \quad (63)$$

we find

$$\begin{aligned} H^I(\mathbf{p}) &= \left[g(\mathbf{p}) - \tilde{V} \sigma_1 \sin p_y + \tilde{V} \sigma_2 \sin p_x \right. \\ &\quad \left. - \sigma_3 \left[\frac{\omega}{2} - \frac{\sqrt{\pi} \tilde{V}}{2} (\cos p_x + \cos p_y) \right] \right] \end{aligned} \quad (64)$$

$$\tilde{V} = V_{10} e^{-\frac{1}{2}\pi} \sqrt{\pi} \quad (65)$$

The ground state of $H^I(\mathbf{p})$ is our Chern band. The function $g(\mathbf{p})$ affects the energy dispersion of the band, but not the Chern density $\mathcal{B}(\mathbf{p})$.

Though $H^I(\mathbf{p})$ has the form of the Lattice Dirac Model (Eq. 4), it is in the topologically trivial region. This is due to our requirement $\omega > 2\sqrt{\pi}\tilde{V}$ which ensures that the two bands do not touch at $p_x = p_y = 0$, which in turn ensures that the Chern number remains $\mathcal{C} = -1$. Due to the topological triviality of $H^I(\mathbf{p})$ the pseudo-spin $\mathbf{n}(\mathbf{p}) = \langle u(\mathbf{p}) | \boldsymbol{\sigma} | u(\mathbf{p}) \rangle$ never enters the southern hemisphere. Nonetheless the overall $\mathcal{C} = -1$ because *nontrivial topology is contained in the \mathbf{p} -dependent basis functions*. Whereas in the traditional lattice Dirac model, the tight binding wavefunctions are \mathbf{p} -independent spinors, $[1, 0]^T$ and $[0, 1]^T$, here they are the states $|\mathbf{p}, n = 0, 1\rangle$ with topologically nontrivial \mathbf{p} dependence. The total \mathcal{B} in this problem has a constant piece $-\frac{1}{2\pi}$ coming from the basis functions and responsible for $\mathcal{C} = -1$, and two more \mathbf{p} -dependent terms with zero integrals: one due to the \mathbf{p} -dependence of the ground state spinor, and a cross term that arises because $\langle n | \nabla_{\mathbf{p}} | n' \rangle \neq 0$ for $n \neq n'$. The total $\mathcal{B}(\mathbf{p})$ is shown in Figure 2 along with the Chern density for the Lattice Dirac Model at $M = 1$. Notice the strong similarity even in this minimal model with just two LLs and one harmonic in V .

Now that we have a nontrivial Chern band with a nonconstant $\mathcal{B}(\mathbf{p})$ let us proceed to the CF-substitution, which will in turn lead us to the gapped state in the Hartree-Fock approximation at $\nu = \frac{1}{3}$ when interactions are turned on.

First we need to find ρ_{FCB} , the projection of the electron density operator to the Chern band. When $V_{10} = 0$, clearly $\rho_{FCB}(\mathbf{q}) = \rho_{LLL}(\mathbf{q})$. To find out what it is when V_{10} is turned on we proceed as follows:

- Find the 2×2 matrix that describes the electron density $\rho_e(\mathbf{q}) = e^{i\mathbf{q} \cdot \mathbf{r}_e}$ in the space of the LLs, $n = 0, 1$.
- Find the eigenstates of $H^I(\mathbf{p})$.
- Project $\rho_e(\mathbf{q}) = e^{i\mathbf{q} \cdot \mathbf{r}_e}$ to the ground state at each \mathbf{p} , our Chern band.

Consider each step in turn. First we find the matrix elements of $\rho_e(\mathbf{q}) = e^{i\mathbf{q} \cdot \mathbf{r}_e}$ between the magnetic Bloch states defined in Eq. 17, which vanish unless the initial momentum \mathbf{p} and final momentum \mathbf{p}' , both restricted to the Brillouin Zone. Recall that

$$\mathbf{p}' \equiv [\mathbf{p} + \mathbf{q}] = (\mathbf{p} + \mathbf{q}) \text{ mod } \mathbf{G} \quad (66)$$

We remind the reader of the definition of $\mathbf{p}' \equiv [\mathbf{p} + \mathbf{q}]$ as the final state momentum brought back to the Brillouin Zone by modding out the appropriate reciprocal lattice vector \mathbf{G} . We are aware that this may not be a standard notation.

The non-zero matrix elements are found to be

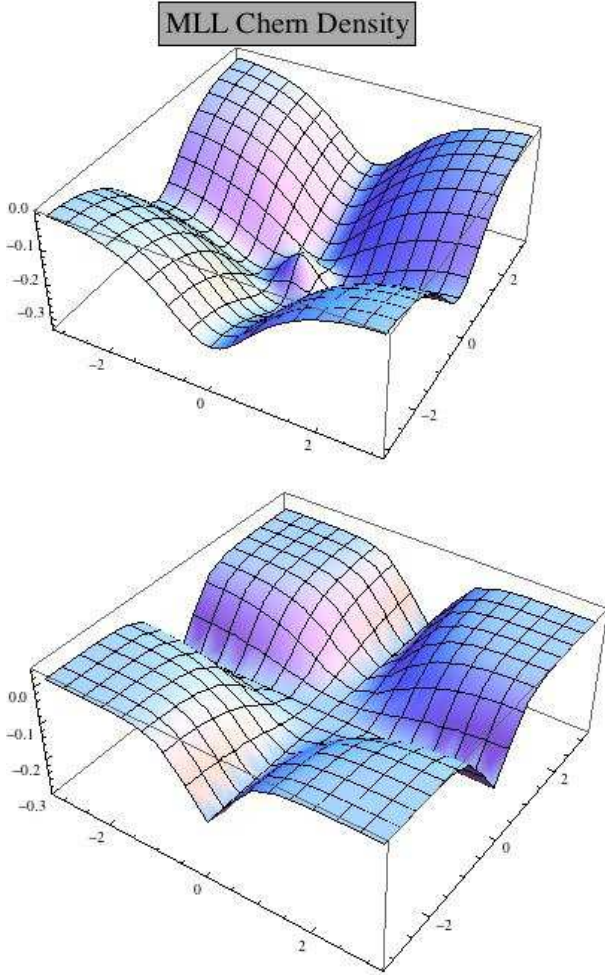


FIG. 2: Top: $\mathcal{B}(\mathbf{p})$ in the lowest band with just two LLs and one harmonic $V_{01} \neq 0$. Bottom: Berry flux density in the lattice Dirac model at $M = 1$.

$$\begin{aligned} \langle [\mathbf{p} + \mathbf{q}] n_2 | e^{i\mathbf{q} \cdot \mathbf{r}_e} | \mathbf{p} n_1 \rangle &= \\ \rho_{n_2 n_1} \exp \left[\frac{i}{2\pi} \left(\frac{1}{2} q_x q_y + q_x p_y - (p_x + q_x) 2\pi N_y \right) \right] & \\ \equiv \rho_{n_2 n_1}(\mathbf{q}) e^{i\Phi(\mathbf{q}, \mathbf{p})} & \end{aligned} \quad (67)$$

where $\rho_{n_2 n_1}(\mathbf{q})$ has been defined in Eq. 63. The asymmetry between p_x and p_y in Eq. 67 reflects our choice of the Landau gauge in defining the basis states in Eq. 17.

The corresponding second-quantized operator is

$$\rho_e(\mathbf{q}) = \sum_{\mathbf{p}} \sum_{n_1, n_2=0,1} a_{n_2}^\dagger([\mathbf{p} + \mathbf{q}]) \rho_{n_2 n_1}(\mathbf{q}) a_{n_1}(\mathbf{p}) e^{i\Phi(\mathbf{q}, \mathbf{p})} \quad (68)$$

where a_n and a_n^\dagger are the operators associated with the basis states $|\mathbf{p}n\rangle$.

Now for the second step, which carries out the unitary transformation to the eigenbasis of H^I . Let U be the matrix that diagonalizes $H^I(\mathbf{p})$ in Eq. 64 and relates a_n to the d_n associated with the energy eigenstates as follows

$$\begin{pmatrix} a_0(\mathbf{p}) \\ a_1(\mathbf{p}) \end{pmatrix} = \begin{pmatrix} U_{00} & U_{01} \\ U_{10} & U_{11} \end{pmatrix} \begin{pmatrix} d_0(\mathbf{p}) \\ d_1(\mathbf{p}) \end{pmatrix} \quad (69)$$

Since $H^I(\mathbf{p})$ is topologically trivial, U , like the eigen-spinors, is globally defined in the Brillouin Zone and periodic in \mathbf{p} . Switching to the new basis and projecting to the ground state we obtain

$$\begin{aligned} \rho_{\text{FCB}}(\mathbf{Q}) &= \sum_{\mathbf{p}} d_0^\dagger(\mathbf{p}') d_0(\mathbf{p}) e^{i\Phi(\mathbf{Q}, \mathbf{p})} f(\mathbf{Q}, \mathbf{p}) \\ f(\mathbf{Q}, \mathbf{p}) &= U_{0n'}^\dagger(\mathbf{p}') \rho_{n'n}(\mathbf{Q}) U_{n0}(\mathbf{p}) \end{aligned} \quad (70)$$

Hereafter the subscript on d_0 , indicating that it corresponds to the ground state will be dropped.

Thus we have a Chern band, a non-constant \mathcal{B} and a closed expression for the projected density. The final step before we carry out the CF substitution is to write this density in terms of ρ_{GMP} . Here is an intuitive argument that this can be done. When $V_{10} = 0$, we know $\rho_{\text{FCB}} = e^{-q^2 l^2/4} \rho_{\text{GMP}}$. As we turn on V_{10} , the perturbing terms are of the form $e^{i\mathbf{G}_0 \cdot \mathbf{r}_e} = e^{i\mathbf{G}_0 \cdot \boldsymbol{\eta}_e} e^{i\mathbf{G}_0 \cdot \mathbf{R}_e}$ where $\mathbf{G}_0 = 2\pi(\mathbf{e}_x n_x + \mathbf{e}_y n_y)$ with only one of n_x or $n_y = \pm 1$. Given the GMP algebra, the repeated action of this perturbation can only be to turn $\rho_{\text{GMP}}(\mathbf{q})$ into a sum over $\rho_{\text{GMP}}(\mathbf{q} + \mathbf{G})$, where \mathbf{G} is now any reciprocal lattice vector. So we do expect that in the end, even for an arbitrary periodic potential

$$\rho_{\text{FCB}}(\mathbf{Q}) = \sum_{\mathbf{G}} c(\mathbf{G}, \mathbf{Q}) \rho_{\text{GMP}}(\mathbf{Q} + \mathbf{G}) \quad (71)$$

Since the bands never touch, perturbation theory will always converge. However the final result is non-perturbative and follows simply from the dependence of $H^I(\mathbf{p})$ on $e^{i\mathbf{G}_0 \cdot \mathbf{R}_e}$. Given the $f(\mathbf{Q}, \mathbf{p})$ of Eq. 70, it is straightforward to find the coefficients $c(\mathbf{G}, \mathbf{Q})$.

The commutators of the projected electron density $\rho_{\text{FCB}}(\mathbf{Q})$ can be worked out, if desired. They will be neither pretty nor universal²⁰, unlike the magnetic translation algebra²¹, depending instead on the details of the lattice via $f(\mathbf{Q}, \mathbf{p})$.

Having expressed $\rho_{\text{FCB}}(\mathbf{Q})$ in terms of $\rho_{\text{GMP}}(\mathbf{Q} + \mathbf{G})$ we need to do the same for a term in \bar{H} that is absent in the usual LLL: the non-constant kinetic energy $-\varepsilon(\mathbf{p})$ of the Chern band. As described earlier, this is a special case ($\mathbf{Q} = 0$) of the Fourier transform we carried out for $\rho_{\text{FCB}}(\mathbf{Q})$.

Note that the phase factor

$$e^{i\Phi(\mathbf{Q}, \mathbf{p})} = \exp \left[\frac{i}{2\pi} \left(\frac{1}{2} Q_x Q_y + q_x p_y - (p_x + Q_x) 2\pi N_y \right) \right] \quad (72)$$

jumps in \mathbf{p} space for a fixed \mathbf{Q} . For example if $\mathbf{Q} = 3\mathbf{e}_y$ and the Brillouin Zone is in the interval $[0 - 2\pi]$ in both directions, then for any \mathbf{p} with $p_y > 2\pi - 3$, adding \mathbf{Q} will take it to the next Brillouin Zone and N_y will have to jump from 0 to 1 to bring \mathbf{p}' within the Brillouin

Zone. Luckily, this discontinuous Φ and its jump are shared by both $\rho_{\text{MLL}}(\mathbf{Q})$ and $\rho_{\text{GMP}}(\mathbf{Q} + \mathbf{G})$. This ensures rapid convergence of the Fourier expansion of the jump-free part $f(\mathbf{Q}, \mathbf{p})$ in Eq. 58.

B. The CF substitution

Now we must switch to CFs. We only sketch the broad ideas. We first consider the case of $\nu = \frac{1}{3}$ when the CF has a charge $e^* = \frac{1}{3}e$ and $l^{*2} = 3l^2 = \frac{3}{2\pi}$. The spatial unit cell is 3 units long in the x-direction so as to enclose unit flux *as seen by the CF* so that the Brillouin Zone of the CF goes from $-\frac{\pi}{3} \leq p_x \leq \frac{\pi}{3}$ and is unchanged in the y-direction. However when we construct the projected electron density operators we will need to consider \mathbf{Q} that runs over the Brillouin Zone of the electron not the CF.

Consider $\rho_{\text{GMP}}(\mathbf{Q})$ which was $e^{i\mathbf{Q}\cdot\mathbf{R}_e}$ in first quantization and which we repeat here for convenience

$$\rho_{\text{GMP}}(\mathbf{Q}) = \sum_{\mathbf{p} \in \text{BZ}_e} d^\dagger(\mathbf{p}')d(\mathbf{p}) \times \exp\left[\frac{i}{2\pi}\left(\frac{Q_x Q_y}{2} + Q_x p_y - (p_x + Q_x)2\pi N_y\right)\right] \quad (73)$$

in second quantization. To go to the CF representation means to write

$$e^{i\mathbf{Q}\cdot\mathbf{R}_e} = e^{i\mathbf{Q}\cdot(\mathbf{R} + \boldsymbol{\eta}c)} \quad (74)$$

in first quantization and the following representation in terms of CF operators C and C^\dagger in second quantization

$$\rho_{\text{GMP}}(\mathbf{Q}) = \sum_{\mathbf{p} \in \text{BZ}_{CF}} C_{n'}^\dagger(\mathbf{p}')C_n(\mathbf{p})\rho_{n'n}(\mathbf{Q} \rightarrow c\mathbf{Q}, l \rightarrow l^*) \times \exp\left[\frac{3i}{2\pi}\left(\frac{1}{2}Q_x Q_y + Q_x p_y - (p_x + Q_x)2\pi N_y\right)\right] \quad (75)$$

where $C_n(\mathbf{p})$ is the canonical CF destruction operator in the CF BZ in the n^{th} CF-Landau level, the 3 is due to $l^{*2} = 3l^2 = \frac{3}{2\pi}$, and the argument of $\rho_{n'n}$ is $\mathbf{Q}c$ because the c in $\boldsymbol{\eta}c$ may be lumped with \mathbf{q} (see Eq. 42 and Eq. 63). Note that all CF-LLs ($n = 0, 1, \dots$) appear in the density, a result of the enlarged Hilbert space in which we are representing the problem.

With the Hamiltonian expressed in terms of CF operators, we move to the Hartree-Fock calculation. We set $\omega = 10$ (the gap between the two electronic LLs) and choose the periodic potential to be $V_{\text{FP}} = V_{10}e^{-\frac{1}{2}\pi} = 1$. We keep 3 CF-LLs which get mixed by the periodic potential and interaction. We end up with three bands which are fairly well separated. Unlike in the continuum where the CF-LLs were uniformly filled, the occupation number here varies with \mathbf{p} (due to the periodic potential) and has to be found self-consistently. Figure 3 shows the

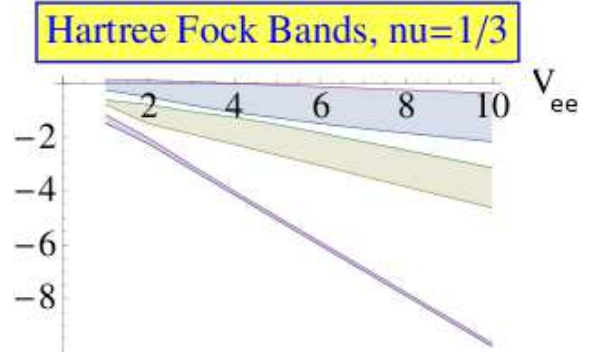


FIG. 3: The results of our Hartree-Fock calculation at $\nu = \frac{1}{3}$ and $\omega = 10$, for the Coulomb interaction $\frac{2\pi V_{ee}}{Q}$. The three bands resulting from three CF-LLs which get mixed and modulated by the periodic potential $V_{\text{FP}} = 1$.

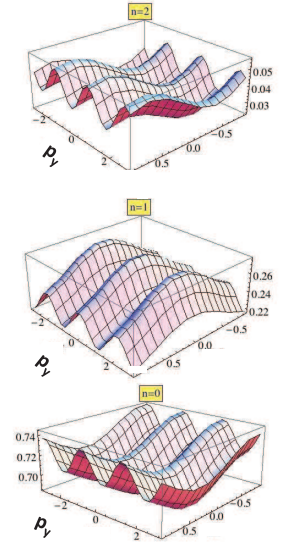


FIG. 4: The occupation numbers in CF-LLs 0,1, and 2 at $V_{ee} = 10, V_{\text{FP}} = 1, \omega = 10$. Notice that the $n = 0, 1$ levels (bottom two) saturate the occupancy while the $n = 2$ (top) level is practically empty, validating the truncation at three CF-LLs and establishing CF theory as a good low-energy description. The plots repeat three times in the p_y direction because T_x and T_x^2 commute with H , but do not commute with T_y and add $\frac{2\pi}{3}$ and $\frac{4\pi}{3}$ to p_y , respectively.

results of our calculation for the Coulomb interaction of strength $\frac{2\pi V_{ee}}{Q}$. We see a clear gap separating the lowest band which is fully occupied from the others, even at very small values of V_{ee} .

This is puzzling since one expects the CF-picture to break down for $V_{ee} \ll V_{\text{FP}}$. Upon further investigation we found two signals that point to the breakdown of the CF picture, one internal to the Hartree-Fock approximation and one external.

The internal signal involves the occupation numbers of the CF-LLs in the ground state at each \mathbf{p} . Figure 4 shows that at $V_{ee} = 10$, $n_{\text{CF}} = 0, 1$ are robustly occupied while $n_{\text{CF}} = 2$ has negligible occupancy. Thus our truncation with three CF-LLs is safe, since the $n = 2$ level is not

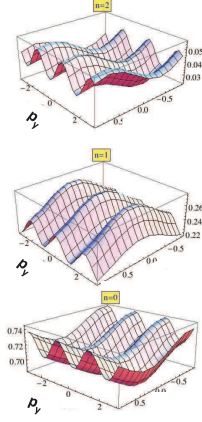


FIG. 5: The occupation numbers in CF-LLs 0,1,and 2 at $V_{ee} = 0.5$, $V_{FP} = 1$, $\omega = 10$. Notice that the particles are levitating towards the $n = 2$ level (top) and moving away from $n = 0$, which calls the truncation at three CF-LLs into question. The plots repeat three times in the p_y direction because T_x and T_x^2 which do not commute with T_y add $\frac{2\pi}{3}$ and $\frac{4\pi}{3}$ to p_y , respectively, commute with H .

called into play. By contrast at $V_{ee} = 0.5$ we see in Figure 5 that occupation of $n_{CF} = 2$ can be substantial. The levitation of the fermions to the upper CF-LLs is a clear indication that CF theory is failing as a good low-energy theory.

Let us observe an interesting three-fold symmetry in the occupations as a function of p_y , which is also reflected in the energy bands. This is a consequence of the x -translation symmetry of the effective CF Hamiltonian³⁵, which, as we recall, has one unit of effective flux per three original (electronic) unit cells. Recall that T_x commutes with the Hamiltonian, but not with T_y . It can be easily shown that

$$T_x |p_x, p_y, n\rangle = e^{i\phi(\mathbf{p})} |p_x, p_y - \frac{2\pi}{3}, n\rangle \quad (76)$$

This symmetry is also possessed by the Hartree-Fock Hamiltonian

$$T_x^\dagger H_{HF}(p_x, p_y) T_x = H_{HF}(p_x, p_y - \frac{2\pi}{3}) \quad (77)$$

and thus by the energy bands and the occupations.

Now we turn to the external test that signals the breakdown of the CF state and is sharper than the one based on occupation numbers. It involves the comparison of the variational energy per particle in the fractional Chern insulator state and the electronic Fermi liquid state.

As mentioned at the end of Section III, despite the fact that we are working in an enlarged space, the ground state energy is variational. Fig. 6 shows the the Hartree-Fock energy per particle of the Fermi liquid (smaller dots) versus to $\frac{1}{3}$ fractional Chern insulator state (larger dots). We see that the Fermi liquid yields to the fractional Chern insulator state at $V_{ee} \simeq 2.5$. We caution the reader that this does not mean that the fractional

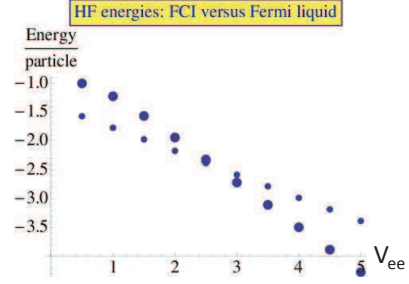


FIG. 6: Comparison of the Hartree-Fock energy per particle of the electronic Fermi liquid (smaller dots) versus the $\frac{1}{3}$ Fractional Chern Insulator state (larger dots). We see that the Fermi liquid, which wins at small interaction strength V_{ee} yields to the fractional Chern insulator state around $V_{ee} = 2.5$.

Chern insulator state unequivocally wins. It is possible that there are correlated *electronic* states with an even lower energy than our CF-state.

To summarize, we produced a non-trivial Chern band by transferring the topology to the basis functions in \mathbf{p} space. These functions arose from two electronic LLs mixed by a periodic potential. The projected charge density at momentum \mathbf{Q} was then written as a computable sum over \mathbf{G} of GMP densities at $\mathbf{Q} + \mathbf{G}$. The GMP densities were treated in the Hamiltonian method by the replacement $\mathbf{R}_e = \mathbf{R} + \eta\mathbf{c}$. Finally a Hartree-Fock calculation was carried out using a gapped CF ground state. We see that although a fractional Chern insulator state always exists, even for very weak interactions V_{ee} , the occupations of the higher CF-LLs becomes smaller with increasing V_{ee} , providing an internal signal of its stability. A sharper limit for the goodness of the fractional Chern insulator state is provided by the comparison to the variational energy of the electronic Fermi liquid state, which wins for $V_{ee} < 2.5$, but gets bested by the fractional Chern insulator state for larger V_{ee} .

C. A digression on LL based bands

A natural extension of the above example is to impose more complicated periodic potentials to get more complicated $\mathcal{B}(\mathbf{p})$ s. Earlier in our exploration⁴² we pursued this line of thought so as to reproduce the $\mathcal{B}(\mathbf{p})$ of some specific lattice model, say the lattice Dirac model. (We see in Fig. 2 that the $\mathcal{B}(\mathbf{p})$ of our Landau level based Chern band with just one harmonic is already not too different from that of the lattice Dirac model.) Our motivation was as follows. *Let us take the view that the FCB problem is defined by (i) $\mathcal{B}(\mathbf{p})$ and (ii) the interaction written in terms of the projected density $\rho_{FCB}(\mathbf{q})$.* The logic be-

hind (i) is that the projected electron coordinate

$$(R_\mu^{FCB})_{\mathbf{p}\mathbf{p}'} = \left(i\frac{\partial}{\partial p_\mu} + \mathcal{A}_\mu(\mathbf{p})\right)\delta^2(\mathbf{p} - \mathbf{p}') \quad (78)$$

has commutators defined by \mathcal{B} :

$$[R_x^{FCB}, R_y^{FCB}]_{\mathbf{p}\mathbf{p}'} = i\mathcal{B}(\mathbf{p})\delta^2(\mathbf{p} - \mathbf{p}') \quad (79)$$

It follows that if we can construct a surrogate band with the same $\mathcal{B}(\mathbf{p})$ as in a given FCB, *then any function of the projected electron coordinates will be algebraically the same in the two problems.*

Let us review where this line of thought leads in the continuum FQH problem. There we represent the electron's projected coordinate \mathbf{R}_e in terms of CF variables \mathbf{R} and $\boldsymbol{\eta}$. Getting the algebra of \mathbf{R}_e correctly also means getting the algebra of ρ_{LLL} , the projected density right, up to a known prefactor. Thus, if $\langle \dots \rangle$ denotes averages in the target band, which here is the LLL,

$$\mathbf{r}_e = \mathbf{R}_e + \boldsymbol{\eta}_e \quad \text{which implies} \quad (80)$$

$$\langle \mathbf{r}_e \rangle = \mathbf{R}_e \quad \text{while} \quad (81)$$

$$\langle e^{i\mathbf{q}\cdot\mathbf{r}_e} \rangle = \langle e^{i\mathbf{q}\cdot(\mathbf{R}_e + \boldsymbol{\eta}_e)} \rangle \quad (82)$$

$$= \langle e^{i\mathbf{q}\cdot\boldsymbol{\eta}_e} \rangle e^{i\mathbf{q}\cdot\mathbf{R}_e} \quad (83)$$

$$= e^{-q^2 l^2/4} e^{i\mathbf{q}\cdot\langle \mathbf{r}_e \rangle} \quad (84)$$

In other words, the projection of the exponential of \mathbf{r}_e is, up to a known prefactor $e^{-q^2 l^2/4}$, the same as the exponential of the projection because $\boldsymbol{\eta}_e$ and \mathbf{R}_e commute. This is why if the projected coordinate is faithfully represented, so is the projected density. We go over these well known facts to highlight the unusual simplicity of projecting to the LLL.

Unfortunately, in the generic FCB problem this is no longer true. Let us define two different projected densities in the FCB. One is the usual one:

$$\rho_{\text{FCB}}(\mathbf{q}) = \langle \text{FCB} | e^{i\mathbf{q}\cdot\mathbf{r}_e} | \text{FCB} \rangle \quad (85)$$

This is the projected density which enters the interacting Hamiltonian in the FCB.

The other is the analogue of the guiding center density:

$$\bar{\rho}_{\text{FCB}}(\mathbf{q}) = e^{i\mathbf{q}\cdot\mathbf{R}_e^{\text{FCB}}} \quad (86)$$

In the FCB problem

$$\rho_{\text{FCB}}(\mathbf{q}) \neq C(q)\bar{\rho}_{\text{FCB}}(\mathbf{q}) \quad (87)$$

because the ‘‘guiding center’’ coordinates \mathbf{R}^{FCB} do not commute with the analogue of the cyclotron coordinates. *Thus, $\mathcal{B}(\mathbf{p})$ is not enough to specify the interacting Hamiltonian in the FCB completely. One needs the expression for $\rho_{\text{FCB}}(\mathbf{Q})$ as well.*

However, to lowest order in \mathbf{q} and \mathbf{q}' we have, in first quantization and in \mathbf{p} -space,

$$[\rho_{\text{FCB}}(\mathbf{q}), \rho_{\text{FCB}}(\mathbf{q}')] = -i[\mathbf{q} \times \mathbf{q}'] \mathcal{B}(\mathbf{p}) + \text{higher order terms} \quad (88)$$

as pointed out by Parameswaran *at al*²⁰.

So if the Chern flux density $\mathcal{B}(\mathbf{p})$ of the surrogate band matches that of the lattice FCB, $\rho_{\text{FCB}}(\mathbf{Q})$ and $\bar{\rho}_{\text{FCB}}(\mathbf{Q})$ will bear a close resemblance to each other but not be equal in all respects. Since these are both models anyway, one may argue that it is sufficient to get a surrogate that approximates the original lattice model and is yet amenable to analytic treatment. However we will not pursue this approach further since there is a more direct way to obtain $\rho_{\text{FCB}}(\mathbf{Q})$ in terms of $\rho_{\text{GMP}}(\mathbf{q} = \mathbf{Q} + \mathbf{G})$ for an arbitrary lattice model, Eq. 54, one of the central claims of this paper.

D. Lattice Chern bands

In the previous section we showed how to carry out the CF substitution in LL-based models with nonconstant $\mathcal{B}(\mathbf{p})$. In this section we consider the lattice Dirac model with some interaction V_{ee} .

Here are the concrete set of steps we follow:

- Construct $\rho_{\text{FCB}}(\mathbf{Q})$, the projected density operator in terms of the eigenfunctions of noninteracting lattice Dirac model Hamiltonian $H(\mathbf{p})$ and the operators d and d^\dagger associated with the Chern band at each \mathbf{p} .
- Construct operators obeying the algebra of $\rho_{\text{GMP}}(\mathbf{Q} + \mathbf{G})$ using d and d^\dagger as per Eq. 53. As noted immediately after that equation, this can always be done. To get the best possible results this must be done in $A_y = 0$ gauge.
- Expand as before, using the complete set of N^4 operators $\rho_{\text{GMP}}(\mathbf{Q} + \mathbf{G})$:

$$\rho_{\text{FCB}}(\mathbf{Q}) = \sum_{\mathbf{G}} c(\mathbf{G}, \mathbf{Q}) \rho_{\text{GMP}}(\mathbf{Q} + \mathbf{G}). \quad (89)$$

This will be just a Fourier expansion in $e^{ip_x n_y - ip_y n_x}$.

- Carry out the CF substitution in ρ_{GMP} and go on to the Hartree-Fock approximation.

We illustrate the above steps with the lattice Dirac model at $M = 1$:

$$H(\mathbf{p}) = \sigma_1 \sin p_x + \sigma_2 \sin p_y + \sigma_3 (1 - \cos p_x - \cos p_y) \quad (90)$$

with ground-state energy

$$-\varepsilon(\mathbf{p}) = -\sqrt{1 + 2(1 - \cos p_x)(1 - \cos p_y)}. \quad (91)$$

The generic formula for the projected charge density is

$$\rho_{\text{FCB}}(\mathbf{Q}) = \sum_{\mathbf{p}} d^\dagger([\mathbf{p} + \mathbf{Q}]d(\mathbf{p})\langle[\mathbf{p} + \mathbf{Q}]|\mathbf{p}\rangle) \quad (92)$$

where d^\dagger, d create and destroy the ground state and $|\mathbf{p}\rangle$ is the corresponding Bloch spinor. However $|\mathbf{p}\rangle$ is not globally defined⁴¹ over the Brillouin Zone because $\mathcal{C} = -1$. Here are two choices that work in two different patches:

$$|\mathbf{p}\rangle_1^0 = \begin{pmatrix} \sin \frac{\theta(\mathbf{p})}{2} \\ -\cos \frac{\theta(\mathbf{p})}{2} e^{i\phi(\mathbf{p})} \end{pmatrix} \quad (93)$$

$$|\mathbf{p}\rangle_2^0 = \begin{pmatrix} \sin \frac{\theta(\mathbf{p})}{2} e^{-i\phi(\mathbf{p})} \\ -\cos \frac{\theta(\mathbf{p})}{2} \end{pmatrix} \quad (94)$$

where

$$\cos \theta(\mathbf{p}) = \frac{1 - \cos p_x - \cos p_y}{\varepsilon(\mathbf{p})} \quad (95)$$

$$e^{i\phi(\mathbf{p})} = \frac{\sin p_x + i \sin p_y}{\sqrt{\sin^2 p_x + \sin^2 p_y}} \quad (96)$$

The superscript 0 on the kets reminds us that these are going to be transformed to a more appropriate gauge later.

The angle $\phi(\mathbf{p})$ is ill defined at $\theta(\mathbf{p}) = 0, \pi$. At $\theta(\mathbf{p}) = 0$, choice $|\mathbf{p}\rangle_2^0$ is good because the component $\sin \frac{\theta(\mathbf{p})}{2} e^{-i\phi(\mathbf{p})}$ vanishes. In a patch where $\theta(\mathbf{p}) = \pi$, the choice $|\mathbf{p}\rangle_1^0$ is good. Figure 7 shows that there are four trouble spots: $(0, 0)$ where the spinor is at the south pole $\theta = \pi$, and points $(0, \pi), (\pi, \pi)$ and $(\pi, 0)$ where it is at the north pole $\theta = 0$. We pick the Brillouin Zone in the range $[-\frac{\pi}{2}, \frac{3\pi}{2}]$ so that the trouble spots are not at the edges. Patch 1 is indicated by the solid right triangle and patch 2 is the rest.

The corresponding Berry connections are

$$\mathcal{A}_1^0(\mathbf{p}) = -\frac{1}{2}(1 + \cos \theta(\mathbf{p}))\nabla\phi \quad (97)$$

$$\mathcal{A}_2^0(\mathbf{p}) = \frac{1}{2}(1 - \cos \theta(\mathbf{p}))\nabla\phi \quad (98)$$

Once again the superscript 0 on the \mathcal{A} 's above signals that this is not yet the final gauge.

If we imagine the edges of the Brillouin Zone parallel to \mathbf{e}_y glued together to form a cylinder and then the top and bottom sewn together to form the torus, this dark line will mark the boundary between the two regions. The difference between the two connections is $-\nabla\phi$, and the integral around the boundary of $-\frac{1}{2\pi}\nabla\phi$ will yield $\mathcal{C} = -1$.

We now reach the final gauge $\mathcal{A}_y = 0$ as follows. Let

us define

$$\Lambda_1(p_x, p_y) = \int_{-\frac{1}{2}\pi}^{p_y} \mathcal{A}_{1y}^0(p_x, p_y') dp_y' \quad (99)$$

$$\Lambda_2(p_x, p_y) = \Lambda_1(p_x, \frac{\pi}{4} - \frac{p_x}{2}) + \int_{\frac{\pi}{4} - \frac{p_x}{2}}^{p_y} \mathcal{A}_{2y}^0(p_x, p_y') dp_y' \quad (100)$$

$$\chi(p_x) = \phi(p_x, \frac{\pi}{4} - \frac{p_x}{2}) \quad (101)$$

and the following final kets in the two patches

$$|\mathbf{p}\rangle_1 = e^{i\Lambda_1} |\mathbf{p}\rangle_1^0 \quad (102)$$

$$|\mathbf{p}\rangle_2 = e^{i\Lambda_2 + i\chi} |\mathbf{p}\rangle_2^0 \quad (103)$$

In this final gauge, not only is $\mathcal{A}_y = 0$, the two expressions above, $|\mathbf{p}\rangle_1$ and $|\mathbf{p}\rangle_2$, merge seamlessly along the sloped line $p_y = \frac{\pi}{4} - \frac{p_x}{2}$ separating the patches and on the vertical boundaries of the Brillouin Zone, which may be glued to form a cylinder. However between the lines $p_y = -\frac{\pi}{2}$ and $p_y = \frac{3\pi}{2}$ there is a phase mismatch so that we cannot roll the cylindrical Brillouin Zone to a torus without a discontinuity at the seam. This had to be so, for otherwise we would have a fully periodic Bloch function and \mathcal{C} would vanish by Stokes' Theorem⁴¹.

A salient feature of this gauge is that $\rho_{\text{FCB}}(\mathbf{Q})$ in Eq. 92 also has jumps in the sum over \mathbf{p} exactly where the $\rho_{\text{GMF}}(\mathbf{Q} + \mathbf{G})$'s do, rendering this the optimal gauge for rapid convergence of the Fourier expansion.

Figure 8 gives a taste of how the Fourier expansion works at a generic value of $\mathbf{Q} = 3\mathbf{e}_x + 3\mathbf{e}_y$. It compares, at fixed $p_x = -\frac{\pi}{2} + 5$, the imaginary part of the

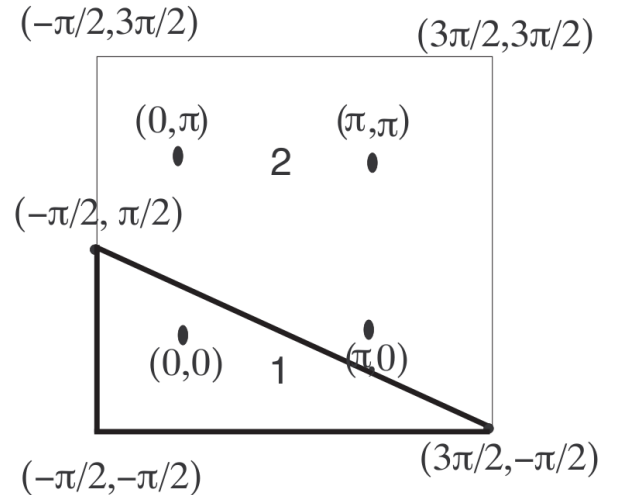


FIG. 7: In patch 1, we have the south pole at $(0, 0)$ and spinor $|\mathbf{p}\rangle_1$ is well defined while in patch 2, spinor $|\mathbf{p}\rangle_2$ is well defined at the north pole reached at the points $(0, \pi), (\pi, 0), (\pi, \pi)$. The patches meet on the right triangle. In the final $\mathcal{A}_y = 0$ gauge the wavefunction is seamless across the hypotenuse $p_y = \frac{\pi}{4} - \frac{p_x}{2}$ and periodic in p_x . However the top and bottom edges differ by a phase and the Chern number is resident in that difference.

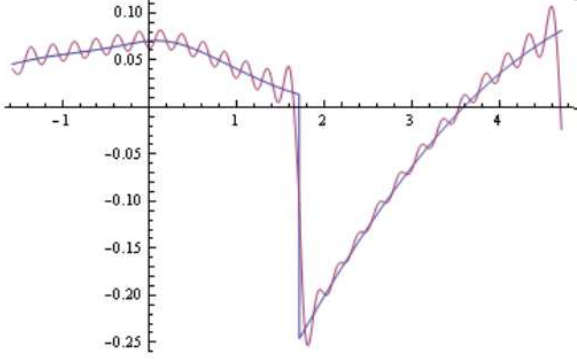


FIG. 8: Here we compare, at fixed $p_x = -\frac{\pi}{2} + 5$, the imaginary part of the coefficient of $d^\dagger([\mathbf{p} + \mathbf{Q}])d(\mathbf{p})$ in $\rho_{\text{FCB}}(\mathbf{Q})$ to the approximation in which the Fourier sum over \mathbf{G} is truncated after 50 harmonics in the p_y direction (from -25 to 25) and 20 in the p_x direction.

coefficient of $d^\dagger([\mathbf{p} + \mathbf{Q}])d(\mathbf{p})$ in $\rho_{\text{FCB}}(\mathbf{Q})$ to the approximation in which the Fourier sum over \mathbf{G} is truncated after 50 harmonics (from -25 to 25) in the p_y direction and 20 in the p_x direction. Note that even though \mathbf{q} has components in both directions, the jump occurs only in the p_y direction due to the periodicity in the p_x direction.

Figure 9 shows the full landscape of the the real part of the coefficient of $d^\dagger([\mathbf{p} + \mathbf{Q}])d(\mathbf{p})$ in $\rho_{\text{FCB}}(\mathbf{Q})$ versus the approximation in which 50 harmonics (from -25 to 25) are kept in the p_y direction and 20 in the p_x direction.

Having expressed everything in terms of $\rho_{\text{GMP}}(\mathbf{Q})$, the the CF substitution and Hartree-Fock analysis can be carried out just as before and we do not discuss it further.

A central message of this work is that since in a problem with $\mathcal{C} \neq 0$, one cannot work with periodic Bloch functions, the expression for $\rho_{\text{FCB}}(\mathbf{Q})$ in the $\mathcal{A}_y = 0$ gauge will necessarily have a jump beyond some p_y depending on q_y when we retract from a point $\mathbf{p} + \mathbf{Q}$ which lies outside the Brillouin Zone to a point $\mathbf{p}' = [\mathbf{p} + \mathbf{Q}]$ within. The GMP density $\rho_{\text{GMP}}(\mathbf{q})$, has a jump at exactly that line and is the right basis to use. When the Chern band supports an fractional Chern insulator, CF coordinates are the natural variables in terms of which the system can be understood in the simplest way.

VI. THE CASE OF TRIVIAL BANDS

Let us ask if we have achieved “too much”. Consider a topologically trivial band with Chern number zero. taking for definiteness the Lattice Dirac Model with $M = 0$. Nothing prevents us from representing its projected density in terms of $\rho_{\text{GMP}}(\mathbf{Q} + \mathbf{G})$

$$\bar{\rho}(\mathbf{Q}) = \sum_{\mathbf{G}} c(\mathbf{G}) \rho_{\text{GMP}}(\mathbf{Q} + \mathbf{G}), \quad (104)$$

and carrying out the CF substitution. So, are there fractional Chern insulators in topologically trivial bands?

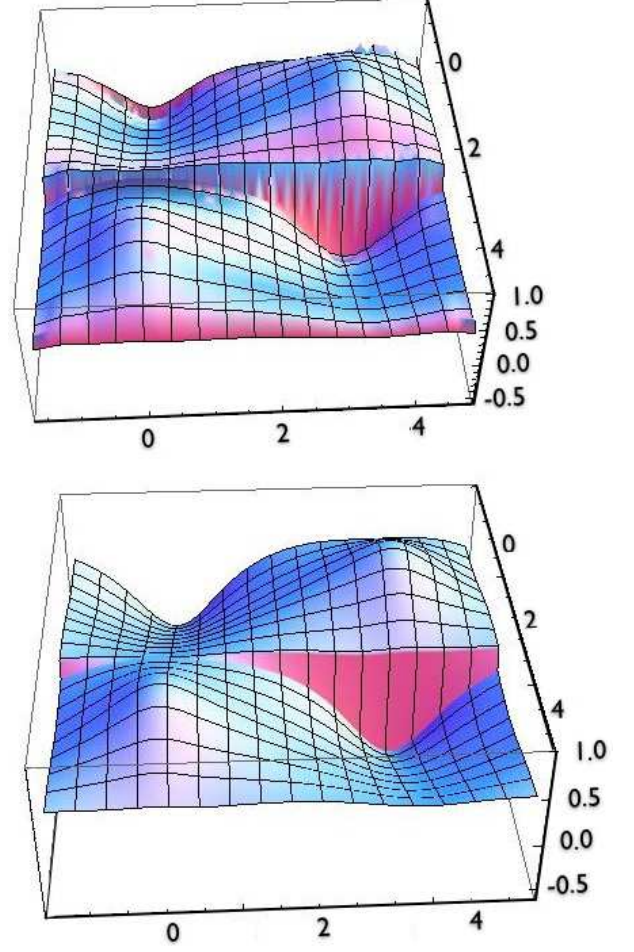


FIG. 9: The upper half shows the full landscape of the real part of the coefficient of $d^\dagger([\mathbf{p} + \mathbf{Q}])d(\mathbf{p})$ in $\rho_{\text{FCB}}(\mathbf{Q})$ in the approximation with 50 harmonics (from -25 to $+25$) in the p_y direction and 20 in the p_x direction. The lower one shows the actual values.

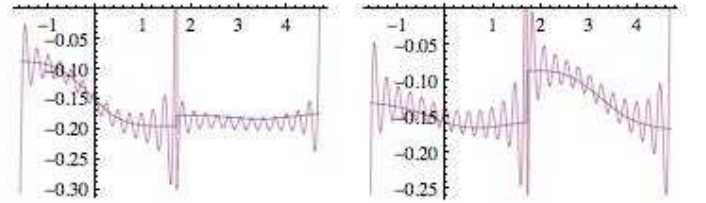


FIG. 10: Comparison, in the case with $\mathcal{C} = 0$ ($M = 3$ in the Lattice Dirac Model), of imaginary parts of exact and approximate densities at $p_x = -\frac{\pi}{2} + 1$ and $p_x = -\frac{\pi}{2} + 6$ with the approximation truncated after 50 harmonics ($+25$ to -25) in the p_y direction.

This appears to be a subtle issue. On the face of it, since the Bloch spinor can now be globally defined as a periodic function in the Brillouin Zone, so can ρ_{FCB} , and its expansion in terms of ρ_{GMP} , which has a jump in the Brillouin Zone, seems ill fated. Although completeness assures us that with infinite number of terms we can do it, in order to give the expansion the best chance, we

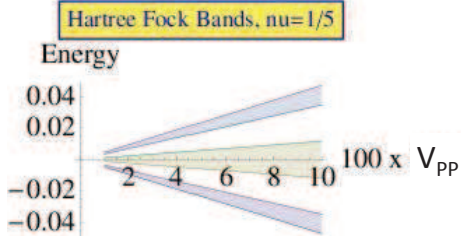


FIG. 11: The highest and lowest energies of the three sub-bands for the exotic fraction $\frac{1}{5}$ as a function of the parameter V_{PP} . The bandwidths grows with the strength of the periodic potential but are still less than the sub-band gaps. The other parameters are $V_{ee} = 1, \omega = 1$.

must first transform the spinor to the gauge $\mathcal{A}_y = 0$, just like the functions entering ρ_{GMP} . This makes $\mathcal{A}_x(p_x, p_y + 2\pi) \neq \mathcal{A}_x(p_x, p_y)$ and causes the familiar jump.

A jump of this sort is inevitable if $B(\mathbf{p})$ is non-constant, because in this gauge

$$\mathcal{A}_x(p_x, p_y) = - \int_{-\frac{\pi}{2}}^{p_y} \mathcal{B}(p_x, p'_y) dp'_y \quad (105)$$

and this integral need not vanish at any fixed p_x .

The Fourier expansion, while not so successful as in the case $\mathcal{C} \neq 0$, is still promising, as shown see Fig. 10 for two slices at $p_x = -\frac{\pi}{2} + 1$ and $p_x = -\frac{\pi}{2} + 6$. The key feature is that the smaller the jump (i.e. the smaller the magnitude of $\mathcal{B}(\mathbf{p})$) the more Fourier components it takes to approximate it to a given accuracy.

The bottom line is that, under certain conditions, even a band with $\mathcal{C} = 0$ could exhibit FQHE under partial filling, an issue we are actively pursuing.

So far we have been able to rule out the following completely trivial case: a band in which $\mathcal{B}(\mathbf{p}) \equiv 0$ with no band dispersion, in which the electrons interact via the Coulomb interaction. The energy is all potential and proportional to V_{ee} . Although an fractional Chern insulator state exists at $\nu = \frac{1}{3}$, its energy is always higher (by a factor of roughly 2) than the energy of the electronic Fermi liquid. Thus, in this case at least, FQHE does not appear to be favoured.

VII. FRACTIONS WHERE $\nu \neq \sigma_{xy}$

In the presence of a periodic potential, the equality $\nu = \sigma_{xy}$ is not mandatory, since Galilean invariance is explicitly broken. Exotic states whose very existence depends on an interplay of interactions and the lattice potential are possible³³. There is suggestive numerical

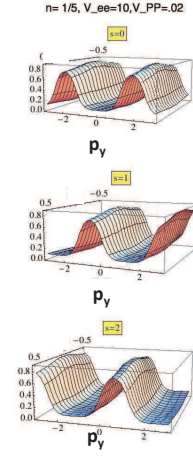


FIG. 12: From the top, the occupation numbers of the three CF-LLL- sub-bands, $s=0,1,2$, for the exotic fraction $\nu = \frac{1}{5}$. The action of $T_x^1, T_x^2, T_x^3, T_x^4$ is to change p_y by multiples of $\frac{6\pi}{5}$ and change the sub-band index by 1 whenever p_y changes by 2π . If the pictures of the three sub-bands are glued together in the order 0, 1, 2, we see 5 oscillations altogether.

evidence for such states in a problem of lattice hard-core bosons in an external field^{44,45}.

Since we have expressed the FCB Hamiltonian in CF language, it is natural for such states to be realized in FCBs under suitable conditions.

Consider a case with $\nu = \frac{1}{5}$. Each electron sees 5 flux quanta. In the continuum, the standard Laughlin/Jain^{9,24} construction involves “attaching” 4 flux quanta per electron, resulting in the CF seeing one unit of effective flux per particle, and filling one CF-LL. Instead, we attach 2 flux quanta to each electron to form CFs. Each CF now sees 3 quanta of effective flux and $\nu^* = \frac{1}{3}$. In the continuum this partially filled CF-LLL is gapless, and thus not stable. However, as we will now show, such a state is generically gapped in the presence of a periodic potential. Since $e^*/e = 3/5$, the CF sees $\frac{3}{5}$ flux quanta in the electronic unit cell. So we must take 5 times the electronic cell (say in the x-direction) to form a CF unit cell that encloses integer flux (3) and ensures that the CF translation operators T_x^5 and T_y commute. In general if there are p/q quanta of effective flux per unit cell, each CF-LL will split into p sub-bands³. Thus, in our example each CF-LL will split into three sub-bands, numbered $s = 0, 1, 2$. If the lowest of these three sub-bands, when filled, is separated from the others by a gap, we obtain a fractional Chern insulator.

Our numerical work fully corroborates this picture. We work to linear order in the periodic potential V_{PP} , and keep only the lowest CF-LL. Note that the treatment is not perturbative in the interaction strength. Fig. 11 shows the three sub-bands whose widths grow with the strength of the periodic potential while the gaps grow even faster. Figure 12 is very interesting. Once again $T_x^1, T_x^2, T_x^3, T_x^4$ commute with H but not T_y . Each power of T_x changes p_y by $\frac{6\pi}{5}$. Starting with $p_y = -\pi$ of the sub-band $s = 0$, if we act with these powers of T_x , we

move to $s = 1$ when the momentum change is $> 2\pi$, and to $s = 2$ when the momentum change is $> 4\pi$. If the three pictures are glued end to end, we see 5 full oscillations. (Compare this to the $\nu = \frac{1}{3}$ case where three periods occurred within the same CF-LL whereas here the 5 oscillations are spread over 3 sub-bands.)

What will be the Hall conductance of this state? We know from Kol and Read³³ that

$$\sigma_{xy} = \frac{\sigma_{\text{CF}}}{1 + 2\sigma_{\text{CF}}} \quad (106)$$

where σ_{CF} , the dimensionless CF Hall conductance of the filled sub-band could be any integer. (When a LL splits into sub-bands we only know that the sum of the Chern numbers of the sub-bands equals that of the original LL.) But no matter what this integer is, the possible values of $\sigma_{xy} = \frac{1}{3}, \frac{2}{5}, \frac{3}{7}..$ do not include $\frac{1}{5}$. The actual value happens to be $\frac{2}{5}$ because $\sigma_{\text{CF}} = 2$.

It is interesting to put these states in the context of what is known previously in the QH regime. It has long been known that in a noninteracting electron problem in a uniform external magnetic flux, with a periodic potential such that a rational number p/q quanta of flux penetrate each unit cell, each band α is characterized by two Chern indices^{3,43} $\sigma_{xy,\alpha}$, m_α which satisfy a Diophantine equation $p\sigma_{xy,\alpha} + qm_\alpha = 1$. Here $\sigma_{xy,\alpha}$ is the Chern number of the band (also the dimensionless Hall conductance). The sum $M = \sum_\alpha m_\alpha$ is the charge transported per unit cell^{34,43} when the lattice potential adiabatically “dragged” by one lattice unit. States with both σ_{xy} and M nonzero are dubbed Hall Crystals³⁴. Turning on interactions and going to the FQH regime, such states were investigated in the context of anyon superfluid ground states of two-dimensional quantum antiferromagnets on a lattice^{31,32}, and by Kol and Read³³ in the context of the FQH states in a periodic potential. Both the latter used the Chern-Simons approach.

One can think of the states for which the Hall conductivity and filling are unequal as resulting from the stabilization of (fractional) Hall crystals by the lattice potential. Numerically, there is some suggestive evidence⁴⁴ for such ground states in the problem of hard-core bosons on a lattice in an external magnetic field⁴⁵.

VIII. SUMMARY AND OUTLOOK

We have demonstrated here that the Hamiltonian theory of the FQHE²², which was very useful in the continuum, is also effective in describing fractionally filled Chern bands (FCB) that exhibit FQH-like effects. The Hamiltonian theory relies on an exact algebraic mapping that expresses the projected density of the Chern band $\rho_{\text{FCB}}(\mathbf{q})$ in terms of CFs in two steps. First, we express ρ_{FCB} as a linear combination of operators ρ_{GMP} satisfying the magnetic translation algebra²¹. These ρ_{GMP} operators can be constructed solely from the canonical fermion operators of the given band, with no reference to any

Landau levels. Second, we perform the CF substitution in ρ_{GMP} exactly as we did in the continuum theory²². These mappings of operator algebras can be carried out for arbitrary lattice models.

We have illustrated our approach by solving two models. The first model is a $\nu = \frac{1}{3}$ fractional Chern insulator and is adiabatically connected to the continuum Laughlin state at the same filling. The second is a more exotic, $\nu = \frac{1}{5}$ fractional Chern insulator relying on the lattice potential for its very existence³³. Its dimensionless Hall conductance is $\frac{2}{5}$ and not $\frac{1}{5}$ as would be expected in Galilean invariant state. In both cases we have computed the band structure of CFs in the Hartree-Fock approximation.

There are many interesting directions which we intend to pursue in future work. Collective excitations for fractionally filled Chern bands can be computed in a conserving approximation in our approach^{22,29,30,37}, as can finite temperature effects^{22,38}.

A specially interesting case is at $\nu = \frac{1}{2}$ in a FCB. One expects an electronic Fermi liquid at weak coupling and a CF-Fermi liquid²⁸⁻³⁰ at strong coupling. This transition, which we propose to study by our operator-based method, has already been explored in the parton formulation recently⁴⁶.

Let us turn to quasiparticle excitations. In addition to Laughlin-type quasiparticles with fractional charge and statistics, the lattice allows us to consider excitations not conceivable in the continuum, such as those associated with lattice vacancies or dislocations⁴⁷.

As stated in the introduction, fractionally filled 2D time-reversal invariant TIs^{5,13} can be treated by labelling the pair of Chern bands making up the noninteracting TI (with equal and opposite Chern index) by a pseudospin index. There is no requirement of S_z conservation, and the interactions can produce states which can spontaneously break time-reversal, and/or states of the Kol-Read type³³. In fact, in a numerical diagonalization on a small system Neupert *et al*¹³ find a time-reversal-symmetric state in a regime of parameters which has a filling of $\frac{2}{3}$ but a degeneracy of 3 (rather than the degeneracy of $3 \times 3 = 9$ one would expect for “independent” $\nu = \frac{1}{3}$ for each pseudospin) on the torus, suggesting that it could be a Kol-Read³³ type state.

Recently, we noticed the work of Grushin *et al*⁴⁸, who have examined the conditions for the stability of the Fractional Chern insulator, and the work of Chamon and Mudry⁴⁹ which generalizes our central claim, Eq. 54, to arbitrary dimensions, and show that they are a complete set in any even dimension.

We thank the NSF for grants DMR-0703992 and PHY-0970069 (GM), DMR-0103639 (RS), Yong-Baek Kim, Herb Fertig, Sid Parameswaran, and Nick Read for illuminating discussions and Anne-Frances Miller for help with the graphics. We are grateful to Shivaji Sondhi and Sid Parameswaran for urging us to confront the numerics. Finally, we are grateful to the Aspen Center for Physics (NSF 1066293) for its hospitality and facilitating our collaboration.

-
- ¹ F. D. M. Haldane, *Phys. Rev. Lett.*, **61**, 2015, (1988).
- ² G. E. Volovik, *Phys. Lett. A* **128**, 277 (1988); *Sov. Phys. JETP* **67**, 1804 (1988).
- ³ D. J. Thouless, M. Kohmoto, M. P. Nightingale, and M. den Nijs, *Phys. Rev. Lett.*, **49**, 405, (1982).
- ⁴ For reviews see, M. Z. Hasan and C. L. Kane, *Rev. Mod. Phys.* **82**, 3045 (2010); X.-L. Qi and S.-C. Zhang, arXiv:1008.2026, *Rev. Mod. Phys.* **83**, 1057 (2011); M. Koenig, S. Wiedmann, C. Bruene, A. Roth, H. Buhmann, L. W. Molenkamp, X.-L. Qi and S.-C. Zhang, *Science* **318**, 766 (2007).
- ⁵ M. Levin and A. Stern *Phys. Rev. Lett.*, **103**, 196803. 2009.
- ⁶ E. Tang, J. W. Mei and X.-G. Wen, *Phys. Rev. Lett.*, **106**, 236802, (2011).
- ⁷ K. Sun, Z. Gu, H. Katsura and S. Das Sarma, *Phys. Rev. Lett.*, **106**, 236803, (2011).
- ⁸ T. Neupert, L. Santos, C. Chamon, and C. Mudry, *Phys. Rev. Lett.*, **106**, 236804, (2011).
- ⁹ R. B. Laughlin, *Phys. Rev. Lett.*, **50**, 1395 (1983).
- ¹⁰ D. N. Sheng, Z. Gu, K. Sun, L. Sheng, arXiv:1102.2568, *Nature Communications* **2**, 389 (2011).
- ¹¹ N. Regnault and A. Bernevig, arXiv: 1105.4867, *Physical Review X* **1**, 021014 (2011); A. Bernevig and N. Regnault, *Phys. Rev. B* **85**, 075128 (2012).
- ¹² Y.-F. Wang, Z.-C. Gu, C.-D. Gong, and D. N. Sheng arXiv:1103.1686, *Phys. Rev. Lett.* **107**, 146803 (2011).
- ¹³ T. Neupert, L. Santos, S. Ryu, C. Chamon and C. Mudry, *Phys. Rev. B* **84**, 165107 (2011).
- ¹⁴ T. Liu, C. Repellin, A. Bernevig, and N. Regnault, arXiv:1206.2626[cond-mat]
- ¹⁵ X.-L. Qi, arXiv:1105.4298, (2011), *Phys. Rev. Lett.* **107**, 126803, (2011)
- ¹⁶ Yang-Le Wu, N. Regnault, B. Andrei Bernevig, arXiv:1206.5773 (2012).
- ¹⁷ J. Maciejko, X.-L. Qi, A. Karch, and S. C. Zhang, *Phys. Rev. Lett.* **105**, 246809 (2010)
- ¹⁸ B. Swingle, M. Barkeshli, J. McGreevy, and T. Senthil, *Phys. Rev. B* **83**, 195139 (2011).
- ¹⁹ Y.-M. Lu and Y. Ran arXiv:1109.0226, *Phys. Rev. B* **85**, 165134 (2012).
- ²⁰ S. A. Parameswaran, R. Roy and S. L. Sondhi, arXiv:1106.4025, *Phys. Rev. B* **85**, 241308 (R)(2012). See also M. Goerbig, *Eur. Phys. J.*, **85**(1), 15,(2012).
- ²¹ S. M. Girvin, A. H. MacDonald and P. M. Platzman, *Phys. Rev. B* **33**, 2481, (1986).
- ²² G. Murthy and R. Shankar, *Rev. Mod. Phys.* **75**, 1101, (2003).
- ²³ Y.-H. Wu, J. K. Jain, K. Sun, arXiv:1207.4439.
- ²⁴ J. K. Jain, *Phys. Rev. Lett.*, **63**, 199, (1989).
- ²⁵ J. M. Leinaas and J. Myrheim, *Nuovo Cimento* **37B**, 1 (1977). F. Wilczek, *Phys. Rev. Lett.* **48**, 1144, (1982).
- ²⁶ S. C. Zhang, T. H. Hansson and S. A. Kivelson, *Phys. Rev. Lett.*, **62**, 82, (1989).
- ²⁷ A. Lopez and E. Fradkin, *Phys. Rev. B* **44**, 5246, (1991).
- ²⁸ B. I. Halperin, P. A. Lee and N. Read, *Phys. Rev.* **B47**, 7312, (1993); V. Kalmeyer and S.-C. Zhang, *Phys. Rev.* **B46**, 9889, (1992).
- ²⁹ V. Pasquier and F. D. M. Haldane, *Nucl. Phys. B* **516**, 719 (1998).
- ³⁰ N. Read, *Phys. Rev. B* **58**, 16262 (1998).
- ³¹ E. Fradkin, *Phys. Rev. B* **42**, 570 (1990); A. Lopez, A. G. Rojo, and E. Fradkin, *Phys. Rev. B* **49**, 15139 (1994).
- ³² D. Eliezer and G. W. Semenoff, *Annals of Physics* **217**, 66 (1992).
- ³³ A. Kol and N. Read, *Phys. Rev. B* **48**, 8890 (1993).
- ³⁴ Z. Tesanovic, F. Axel, and B. I. Halperin, *Phys. Rev. B* **39**, 8525 (1989); G. Murthy, *Phys. Rev. Lett.* **84**, 350 (2000): *Phys. Rev. Lett.* **85**, 1954 (2000).
- ³⁵ D. Xiao, M. Chang, and Q. Niu, *Rev. Mod. Phys.* **82**, 1959, (2010).
- ³⁶ G. Murthy, K. Park, R. Shankar and J. K. Jain, *Phys. Rev. B* **58**, 15363 (1998); G. Murthy and R. Shankar, *Phys. Rev. B* **59**, 12260 (1999); *Phys. Rev. B* **65**, 245309 (2002).
- ³⁷ G. Murthy, *Phys. Rev. B* **64**, 195310 (2001).
- ³⁸ R. Shankar, *Phys. Rev. Lett.* **84**, 3946 (2000); G. Murthy, *Jour. Phys. Condens. Matter* **12**, 10543 (2000); R. Shankar, *Phys. Rev. B* **63**, 085322 (2001).
- ³⁹ G. Murthy and R. Shankar, *Phys. Rev. B* **76**, 075341 (2007).
- ⁴⁰ G. Murthy, *Phys. Rev. Lett.* **103**, 206802 (2009).
- ⁴¹ D. J. Thouless, *J. Phys.* **C 17**, L325 (1984).
- ⁴² G. Murthy and R. Shankar, arXiv:1108.5501, unpublished.
- ⁴³ A. H. MacDonald, *Phys. Rev. B* **28**, 6713 (1983); I. Dana, Y. Avron, and J. Zak, *J. Phys. C* **18**, L679 (1985); H. Kunz, *Phys. Rev. Lett.* **57**, 1095 (1986).
- ⁴⁴ G. Möller and N. R. Cooper, *Phys. Rev. Lett.* **103**, 105303 (2009).
- ⁴⁵ A. S. Sorensen, E. Demler, and M. D. Lukin, *Phys. Rev. Lett.* **94**, 086803(2005).
- ⁴⁶ M. Barkeshli and J. McGreevy, arXiv:1206.6530[cond-mat].
- ⁴⁷ M. Barkeshli and X.-L. Qi, arXiv:1112.3311.
- ⁴⁸ A. G. Grushin, T. Neupert, C. Chamon, C. Mudry, arXiv:1207.4097.
- ⁴⁹ C. Chamon and C. Mudry, arXiv:1207.6543 (2012).